Front. Mater. Sci. 2025, 19(1): 250717
https://doi.org/10.1007/s11706-025-0717-0

RESEARCH ARTICLE

Surfactant-free emulsion electrospinning of curcumin-loaded poly(ε-caprolactone)/bovine serum albumin composite fibers for biomedical applications

Peng-Hui Zhu, Shu-Hua Teng (✉), and Peng Wang (✉)

School of Materials Science and Physics, China University of Mining and Technology, Xuzhou 221116, China

ABSTRACT: A novel and eco-friendly ethyl acetate/water solvent system was employed to create stable water-in-oil (W/O) emulsions of curcumin (Cur)-loaded poly(ε-caprolactone) (PCL)/bovine serum albumin (BSA) without the need for surfactants. The size of emulsion droplets decreased with the rise of the BSA concentration but increased with the drop of the oil-to-water (OTW) volume ratio. Upon electrospinning, the morphology of Cur-loaded PCL/BSA composites transformed from bead-like structures to uniform fibers as the BSA concentration rose from 0% (w/v) to 10% (w/v). With the enhancement of the OTW volume ratio, the composite fibers displayed an increased diameter and a consistently uniform morphology. The highest modulus of elasticity (0.198 MPa) and the largest elongation at break (199%) of fibers were achieved at the OTW volume ratio of 7:3, while the maximum tensile strength (3.83 MPa) was obtained at 8:2. Notably, the presence of BSA resulted in the superhydrophilicity of composite fibers. Moreover, all composite fibers exhibited sustained drug release behaviors, especially for those with the OTW volume ratio of 7:3, the release behavior of which was the best to match the first-order model. This study is expected to improve biofunctions of hydrophobic PCL and expand its applications in biomedical fields.

KEYWORDS: emulsion electrospinning; surfactant-free emulsion; composite fiber; superhydrophilicity; drug release

Contents

Received October 8, 2024; accepted January 10, 2025

E-mails: shteng425@cumt.edu.cn (S.H.T.), wp425@qq.com (P.W.)

1 Introduction

Emulsion electrospinning has been recognized as a versatile and green technique [1–2] to develop multi-functional nanofibers used in water purification, drug delivery, enzyme immobilization, food packaging, etc. [3–5]. Particularly, emulsion electrospinning allows for the creation of functional composite nanofibers that contain two components with opposite wettability [6–7]. When used as drug carriers, those composite nanofibers are capable of encapsulating bioactive therapeutic agents without affecting their structural characteristics or biological activities [8–10], which will potentially improve the accessibility and regulate the release kinetics of bioactive substances. A crucial step for achievement in emulsion electrospinning is the preparation of a stable emulsion system. To guarantee its stability, surfactants or nanoparticles (NPs) are typically employed as stabilizers. However, the complete removal of such stabilizers from final fiber products is challenging, which may potentially have an effect on both the biocompatibility and the functionality of fibers. Therefore, the exploration of surfactant-free emulsion systems for electrospinning is gaining increasing attention, especially in biomedical applications.

Poly(ε-caprolactone) (PCL), a biodegradable polyester approved by the Food and Drug Administration (FDA), has been extensively used in tissue engineering and drug delivery [11–13]. Nevertheless, its hydrophobic nature is unfavorable to the adhesion and growth of cells, thus posing significant limitations to its broader use in biomedicine. To address this issue, various PCL-based composite fibers with improved hydrophilicity and multiple functions have been developed recently via emulsion electrospinning through blending PCL with hydrophilic substances like ceramics or other polymers [14–16]. For instance, Snyder et al. successfully increased the hydrophilicity of PCL fibers through the integration of nonionic surfactants (sorbitan monooleate and poloxamer) into the formulation [17]. Similarly, Azimi et al. adopted the dry-spinning technique to synthesize PCL fibers with combined hydrophilic–hydrophobic properties through the incorporation of gelatin NPs [18]. Besides, bovine serum albumin (BSA), a water-soluble protein, has been extensively employed in pharmaceutical and biotechnological applications [19–21]. Valmikinathan et al. developed PCL/BSA composite fibers for the controlled release of nerve growth factors (NGFs) via the gradual degradation of BSA [22]. Despite progresses mentioned above, toxic organic solvents like dichloromethane (DCM), trichloromethane (TCM), and hexafluoroisopropanol (HFIP) have been adopted to prepare water-in-oil (W/O) emulsions in most studies, raising concerns about environmental protection and biological safety. Up to now, a prevalent challenge lies in the exploration of green solvents for emulsion electrospinning applied to the fabrication of PCL-based composite fibers with improved hydrophilicity.

Ethyl acetate (EA) is regarded as one of the greenest solvents for electrospinning according to the *GlaxoSmithKline* (*GSK*) *Solvent Sustainability Guide* due to its low toxicity to health, minimal impact on aquatic environment, and high stability [2]. Zhang et al. used EA as a green and suitable solvent for the fabrication of PCL microparticles [23]. Causa et al. prepared PCL films via casting of ethyl lactate and EA mixed solutions [24]. However, EA is not a suitable solvent for electrospinning of PCL, leading to limited research on formulating PCL nanofibers using EA as the solvent.

The objective of the present study is to explore the fabrication of hydrophilic PCL/BSA composite fibers for biomedical applications using EA/water as the benign solvent through a green technique, surfactant-free emulsion electrospinning. Curcumin (Cur) was selected as a model drug for the encapsulation into PCL/BSA composite fibers considering its versatile bioactivities including antioxidant, antibacterial, anti-inflammatory, and antifungal properties [25–26]. Besides being a key component of PCL/BSA composite fibers, BSA also served as a surfactant to maintain the stability of the W/O emulsion system due to its amphiphilic nature, thus eliminating the need for additional surfactants. The influences of both BSA concentration and oil-to-water (OTW) volume ratio on the morphology and stability of emulsions were investigated, too. The combination of hydrophobic PCL with hydrophilic BSA via emulsion electrospinning is expected to be capable of effectively improving the morphology, thermal stability, wettability, mechanical property, and drug release behavior of the obtained composite fibers.

2 Materials and methods

2.1 Materials

BSA powders (pH = 7) with a purity of ⩾ 98% were purchased from Sigma-Aldrich, while PCL (number-average molecular weight (Mn) = 80 000), Cur (98%), EA (analytical reagent (AR), 99%), and all other reagents used in this study were commercially obtained from Shanghai Maclin Biochemical Technology Co., Ltd.

2.2 Preparation of Cur-loaded PCL/BSA emulsions

A clear BSA solution (10% (w/v)) was initially prepared through the complete dissolution of BSA powders in deionized water (DIW), leading to the formation of the water phase. Meanwhile, PCL (15% (w/v)) and Cur (5 wt.% relative to PCL) were simultaneously dissolved in EA to prepare a yellow solution, forming the oil phase. Subsequently, the oil phase and the water phase were mixed according to different OTW volume ratios of 9:1, 8:2, and 7:3, followed by full emulsification at room temperature to finally obtain stable W/O emulsions denoted as Emulsions 9:1, 8:2, and 7:3, and weight proportions of BSA relative to the total weight of the PCL/BSA composite were calculated to be 6.9%, 14.3%, and 22.2%, respectively.

2.3 Electrospinning of emulsions

Each Cur-loaded PCL/BSA emulsion was transferred into a glass syringe and electrospun into fibers under an electrostatic filed of 15 kV/12 cm and with an injection rate of 2.0 mL·h^{-1}. Then, fibers were collected on the aluminum foil followed by placement in the dark with ventilation conditions for one day to ensure complete evaporation of the solvent. For control purposes, Cur-loaded PCL fibers with the OTW volume ratio of 10:0 were also prepared without the addition of the water phase. Additionally, Cur-loaded PCL fibers without BSA were also prepared via replacing the BSA solution with an equal volume of DIW, maintaining the OTW volume ratio of 8:2.

2.4 Characterizations

Emulsion droplets were examined using a Keyence VHX 5000 microscope, followed by estimation of both the average diameter and the size distribution through the measurement of 100 droplets using Nano Measurer 1.2 software. The fiber morphology was observed through field-emission scanning electron microscopy (FE-SEM) on a Hitachi SU8220 SEM instrument, the sample phase composition was investigated via Fourier transform infrared spectroscopy (FTIR) on a PE-983G spectroscope, while differential scanning calorimetry (DSC) was carried out using a STA 449 F3 Jupiter® thermal analyzer at a heating rate of 10 °C·min^{-1}.

2.5 Evaluation on mechanical properties and wettability of composite fibers

Each PCL/BSA fibrous membrane was cut into rectangular specimens (7 cm × 30 cm), and their exact thicknesses were measured using a micrometer. Tensile behaviors of such specimens, with a gauge length of 20 mm, were then evaluated when the speed of the cross-head was 5 mm·min^{-1} using a WDW-5 universal testing machine (UTM). Three samples for each condition were tested, and their mechanical parameters including tensile strength, elastic modulus, and strain at failure were calculated, which were expressed as mean ± standard deviation (SD).

The wettability of any tested fibrous membrane (15 mm × 15 mm) was assessed using a JC2000D2A instrument. Briefly, a drop of DIW was carefully placed onto the membrane surface. After different periods of time, pictures of the water droplet on the surface were taken, followed by the measurement of corresponding contact angles.

2.6 Evaluation on *in vitro* drug release behaviors of composite fibers

For the *in vitro* drug release test, each Cur-loaded fibrous membrane was soaked in a 50 mL phosphate buffered saline (PBS) solution (0.01 mol·L^{-1}, pH 7.4) containing 0.5% (w/v) Tween 80 at 37 °C. After a period of immersion, the supernatant (5 mL) was withdrawn, which was then analyzed using an ultraviolet (UV) spectrophotometer (Evolution 300) at 428 nm, and the concentration of released Cur was calculated based on the linear correlation ($A = 0.0309 + 0.04862C$, $R^2 = 0.9996$) between the Cur concentration (C, unit: μg·ml^{-1}) and the absorbance (A). The average drug concentrations released from fibrous membranes were obtained from triplicate

tests. Several mathematical models (zero-order, first-order, Higuchi, and Hixson–Crowell) were used to analyze the release kinetics of Cur from the composite fibers, and the correlation coefficients (R^2) were obtained from the fitting release profiles to each model.

3 Results and discussion

3.1 Morphology and stability of emulsions

In the present study, a stable W/O emulsion system was developed through mixing the BSA aqueous solution with the Cur-loaded PCL solution in EA without the addition of any extra surfactant. It was observed that the droplet diameter, revealed in Fig. 1, and the average particle size, obtained from the particle size distribution (PSD) profile in Fig. S1 (included by ESM of Appendix), of the Cur-loaded PCL/BSA emulsion decreased with the rise of the BSA concentration from 0% (w/v) to 10% (w/v), demonstrating the superior emulsifying capability of BSA. Figure S2 (included by ESM of Appendix) illustrates the change in the emulsion stability with varying the concentration of BSA. It is observed that the BSA-free oil–water system exhibited significant phase separation after 5 h without stirring, whereas the addition of BSA noticeably enhanced the stability of the emulsion, which might subsequently be formulated into fibers via emulsion electrospinning. Figure 2 shows that the morphology of resultant Cur-loaded PCL/BSA composite fibers was greatly improved through the addition of 10% (w/v) BSA. In contrast, there were some agglomerated beads when BSA was absent. The morphological improvement is mainly attributable to the increase in the emulsion conductivity through the addition of BSA because it ionizes when dissolved in water [27]. The above results suggest that, through the adjustment of the concentration of BSA in the emulsion, the microstructure of PCL/BSA composite fibers can be modified, thereby optimizing their functions for biomedical applications.

In the present emulsion system, amphiphilic BSA serves dual roles: it is not only a component of PCL/BSA composites, but also functions as a surfactant adsorbed at the oil–water interface to stabilize the emulsion. A series of emulsions were formulated at different OTW volume ratios of 9:1, 8:2, and 7:3 with a fixed concentration of BSA at 10% (w/v). As shown in Fig. 3, all three emulsions demonstrate excellent stability, characterized by the uniform dispersion of water droplets within the oil phase. The average sizes of emulsion droplets are determined as (3.85 ± 0.68) μm for Emulsion 9:1, (8.89 ± 2.40) μm for Emulsion 8:2, and (10.75 ± 2.65) μm for Emulsion 7:3,

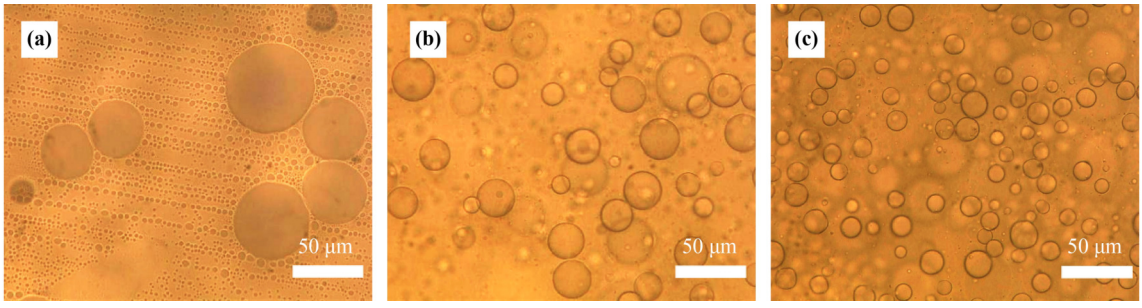

Fig. 1 Micrographs of emulsion droplets obtained with different concentrations of BSA: (**a**) 0% (w/v); (**b**) 5% (w/v); (**c**) 10% (w/v).

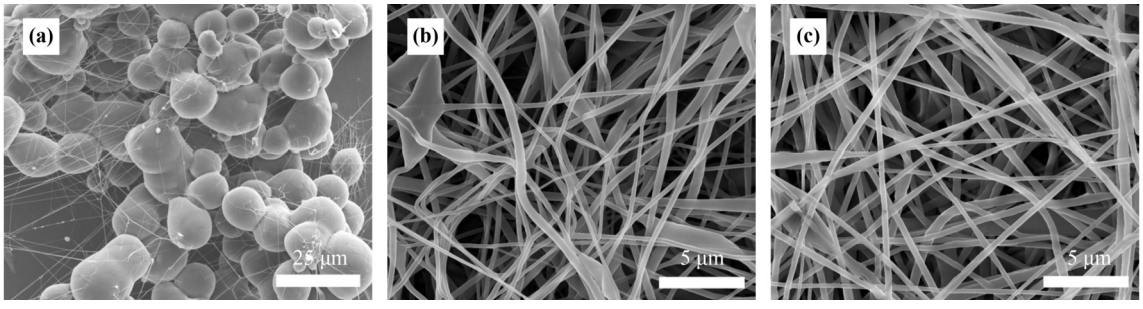

Fig. 2 SEM images of Cur-loaded PCL/BSA composite fibers obtained with different concentrations of BSA: (**a**) 0% (w/v); (**b**) 5% (w/v); (**c**) 10% (w/v).

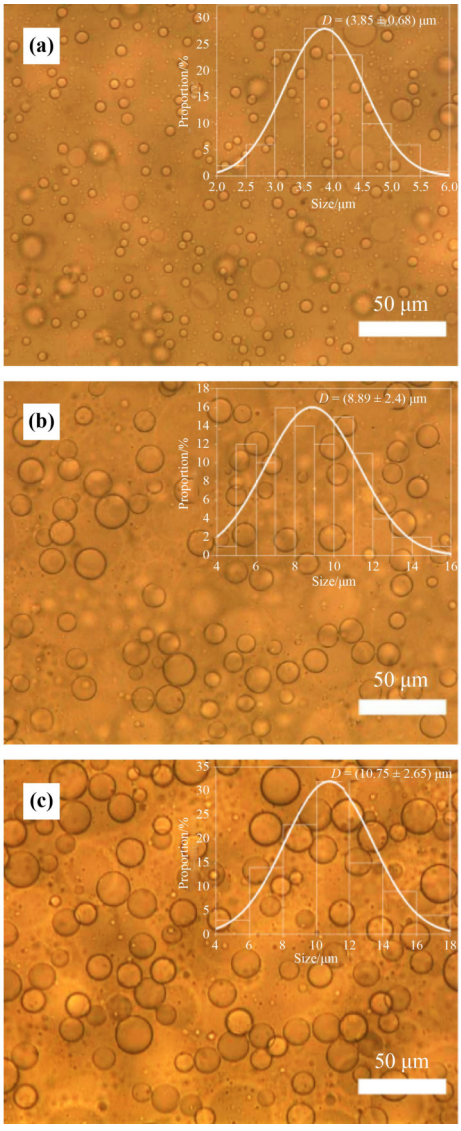

Fig. 3 Microscopic photos of emulsions with different OTW volume ratios of (**a**) 9:1, (**b**) 8:2, and (**c**) 7:3 (insets indicate corresponding PSD profiles).

implying a gradual increase in the droplet size of the emulsion with the decrease in the OTW volume ratio, consistent with the trend observed in our previous study [28], which is primarily attributable to that the reduction in the viscosity of the emulsion system resulting from the decrease in the OTW volume ratio diminishes the homogenization efficiency. In addition, such emulsions maintained high stability even after standing at room temperature for 5 h (Fig. 4), which was adequate for the completeness of the electrospinning process performed in this study. However, after further standing for 24 h, there was some degree of stratification in Emulsions 8:2 and 7:3, while no obvious effect on the stability of Emulsion 9:1. The better long-term stability of the emulsion with a larger

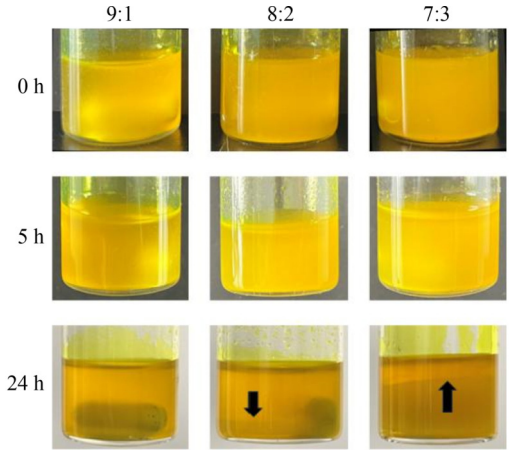

Fig. 4 Stability of emulsions with different OTW volume ratios after standing for different periods of time at room temperature.

OTW volume ratio is likely ascribed to that it can provide a more continuous oil phase for the protection of water droplets from coalescence over time.

3.2 Morphology, compositions, and thermal behaviors of composite fibers

Emulsions with various OTW volume ratios were formulated into Cur-loaded PCL/BMP composite fibers through electrospinning, and the morphologies of as-obtained fibers were displayed in Fig. 5. As apparently revealed in Fig. 5(a), the Cur-loaded PCL solution in neat EA exhibits poor electrospinnability that results in the accumulation of irregular beads, indicating that EA is impossible to be selected as an ideal solvent for the electrospinning of PCL. Notably, the spherical nature of the Cur-loaded PCL sample hinders the formation of the uniform membrane, rendering subsequent property assessments unfeasible. Hence, these results were not included. In contrast, when a 10% (w/v) BSA solution constituted the aqueous phase of the emulsion, all three electrospun samples obtained at different OTW volume ratios presented good fiber morphology, characterized with smooth surfaces and bead-free structures. However, as the OTW volume ratio diminished from 9:1 to 7:3, there was a noticeable rise in the average diameter of fibers from (219.06 ± 77.7) to (567.02 ± 221.01) nm, accompanied by a broadening of the diameter distribution. That was probably due to the corresponding increase in the diameter of emulsion droplets (Fig. 3).

The typical FTIR analysis of the Cur-loaded PCL/BSA (8:2) composite fibers was illustrated in Fig. 6(a). By

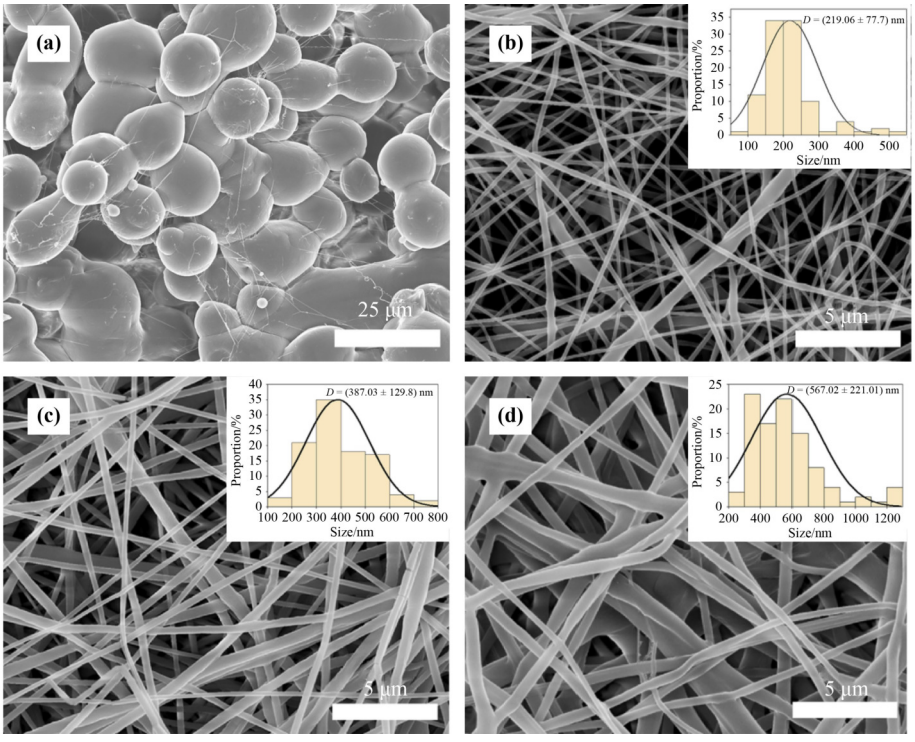

Fig. 5 SEM images of Cur-loaded PCL/BSA composite fibers obtained at different OTW volume ratios: (**a**) 10:0; (**b**) 9:1; (**c**) 8:2; (**d**) 7:3.

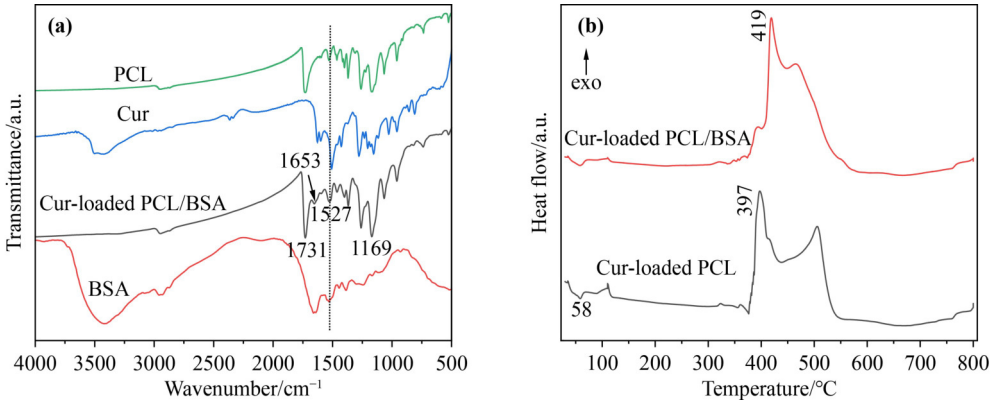

Fig. 6 (**a**) FTIR and (**b**) DSC curves of samples with different compositions.

comparing with spectra of neat PCL, Cur, and BSA, it was speculated that the sharp and strong adsorption peaks at 1731 and 1169 cm^{-1} in the spectrum of composite fibers were assigned to the stretching vibrations of C=O and C−O−C groups in PCL, respectively [29]. The adsorption peak at 1653 cm^{-1} was ascribed to the amide I band of BSA (C=O). The C=O stretching vibration of Cur located at 1510 cm^{-1} was merged with those of PCL (C−O stretching, 1531 cm^{-1}) and BSA (amide II, 1531 cm^{-1}), which resulted in the appearance of a new peak at 1527 cm^{-1} in composite fibers. In addition, the adsorption bands at 3200–3600 cm^{-1} (OH stretching vibrations) of Cur and BSA were not found in Cur-loaded PCL/BSA composite fibers, suggesting a possible interaction among Cur, BSA, and PCL during the fabrication process [30]. Furthermore, it implied from DSC curves in Fig. 6(b) that while the addition of BSA had a mild effect on the melting temperature (58 °C) of Cur-loaded PCL, it greatly enhanced its initial decomposition temperature from 397 to 419 °C, suggesting an improvement in the thermal stability through the combination with BSA.

3.3 Mechanical properties of composite fibers

The stress–strain curves of Cur-loaded PCL/BSA fibrous membranes were determined through tensile testing and plotted in Fig. 7. The results suggested that all three fibrous membranes, regardless of the OTW volume ratio during the fabrication, exhibited a similar stretching behavior: they initially underwent a minor elastic deformation, followed by a yield stage, and ultimately led to fracture. As illustrated in Table 1, both the modulus of elasticity and the ductility of the fibrous membrane gradually rose with the increase in the OTW volume ratio.

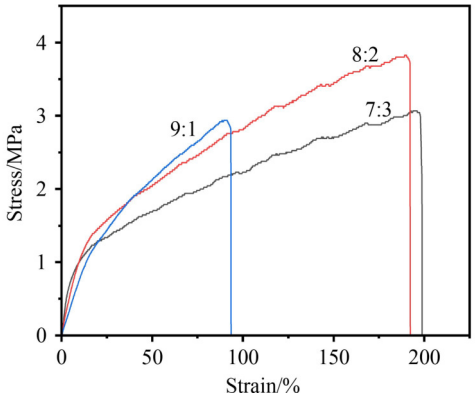

Fig. 7 Stress–strain curves of Cur-loaded PCL/BSA fibrous membranes obtained at different OTW volume ratios.

Table 1 Values of tensile strength, modulus of elasticity, and elongation at break of Cur-loaded PCL/BSA fibrous membranes obtained at different OTW volume ratios

OTW volume ratio	Tensile strength/MPa	Modulus of elasticity/MPa	Elongation at break/%
10:0	–	–	–
9:1	2.98 (± 0.12)	0.074 (± 0.004)	94 (± 1.82)
8:2	3.83 (± 0.23)	0.104 (± 0.008)	193 (± 2.54)
7:3	3.07 (± 0.21)	0.198 (± 0.015)	199 (± 4.05)

This trend can be assigned to the gradual increase in the average diameter of fibers. Specifically, the fibrous membrane with the OTW volume ratio of 7:3 presented both the highest modulus of elasticity (0.198 MPa) and the largest elongation at break (199%). Conversely, the maximum tensile strength of 3.83 MPa was achieved at the OTW volume ratio of 8:2, likely due to a more uniform size distribution and an optimal BSA content within the composite fibers.

3.4 Wettability of composite fibers

The surface wettability of Cur-loaded PCL/BSA composite fibers was assessed through measurements of water contact angles (WCAs). As displayed in Fig. 8(a), water droplets quickly infiltrated into all three composite membranes (9:1, 8:2, 7:3), achieving the WCA of nearly 0° after contact for 3, 5, and 7 s, respectively. Such a rapid infiltration of water indicated the excellent superhydrophilicity of these composite fibers, primarily attributed to the addition of hydrophilic BSA, which was also verified from another perspective by the appearance of large WCA (~75°) on the surface of PCL-Cur fibers obtained in the absence of either the water phase (10:0) or BSA (8:2, BSA-free). In addition, the choice of EA as the solvent in this study might also contribute to the enhancement in hydrophilicity of composite fibers, because the contact angle of PCL-Cur fibers obtained in this study was about 75°, while it was reported by Teodoro et al. that PCL-Cur fabricated using chloroform, but not EA, as the solvent had a contact angle of 117°, exhibiting their hydrophobicity [31]. The improvement in hydrophilicity of PCL fibers through their combination with BSA could potentially facilitate the adhesion and proliferation of cells, thereby offering significant advantages for their

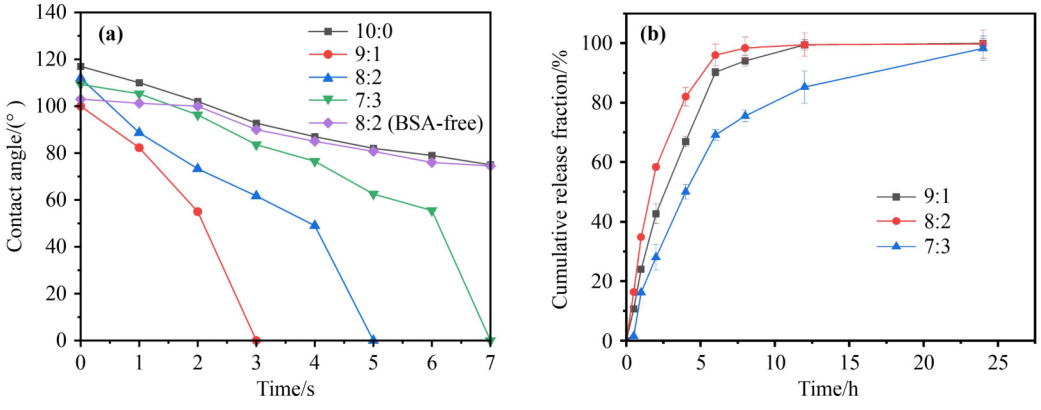

Fig. 8 (**a**) Contact angles and (**b**) drug release profiles of composite membranes obtained at different OTW volume ratios.

applications within the human body.

3.5 *In vitro* release behaviors of Cur from composite fibers

Figure 8(b) illustrates cumulative release profiles of Cur from PCL/BSA composite fibers over time. During the initial 2 h of period, all three samples demonstrated rapid and nearly linear sustained drug release profiles, mainly arising from the abrupt release of Cur particles exposed on the surface of composite fibers. However, the release rate of this initial stage was dependent on the OTW volume ratio, achieving a minimum fraction of 28.0% for PCL/BSA (7:3). In contrast, much higher cumulative release fractions of about 42.6% and 58.3% were obtained during the initial release period for composite fibers with OTW volume ratios of 9:1 and 8:2, respectively. Their larger surface areas associated with smaller average diameters might be responsible for the faster release of drugs exposed on the fiber surface. Afterwards, the drug release decelerated, and the drug concentration eventually reached equilibrium within 24 h due to their good superhydrophilicity. Notably, the PCL/BSA composite fibers with the OTW volume ratio of 7:3 exhibited the most sustained drug release manner without significant burst release, which was likely due to the increased diffusion path length of Cur particles associated with their larger fiber diameter. The sustained release of Cur within 24 h would help to prevent its inactivation when present in the body.

The release mechanism of Cur from PCL/BSA composite fibers was also explored separately using zero-order, first-order, Higuchi, and Hixson–Crowell models, and R^2 values for all models were further summarized in Table 2. Among those four mathematical models, it indicated that the first-order one was the best to be matched with release profiles of Cur from all three PCL/BSA composite fibers, suggesting that the release process was mainly controlled by diffusion. Especially, composite fibers with the OTW volume ratio of 7:3 presented the highest R^2 value (0.99549) for the first-order model. After a rapid release of absorbed Cur molecules from the surface of PCL/BSA composite fibers, the encapsulated drug within fibers would then gradually diffuse through the swollen fiber matrix into the surrounding medium. During this stage, the drug was released at a relatively stable rate and was primarily dominated by two factors in the present system: the hydrophilicity of the composite fibers and the diameter of the fibers. Owing to the endowed superhydrophilicity via the introduction of BSA, the PCL/BSA composite fibers were liable to swell in the PBS medium containing Tween 80, which facilitated the sustained release of the entrapped drug via diffusion. Regarding the effect of the fiber diameter on drug release, Chen et al. found that coarse fibers exhibited a slower rate of drug release as compared to that of fine fibers [32]. Therefore, the more sustained drug release behavior of composite fibers with the OTW volume ratio of 7:3, compared to those of other two samples, was mainly attributed to the presence of farther diffusion paths for the drug from fibers caused by the larger fiber diameter.

Table 2 R^2 values of fitting release profiles for Cur-loaded PCL/BSA composite fibers obtained at different OTW volume ratios corresponding to different kinetics models

OTW volume ratio	R^2			
	Zero-order	First-order	Higuchi	Hixson–Crowell
9:1	0.48992	0.94209	0.74711	0.77435
8:2	0.38199	0.77779	0.65111	0.61526
7:3	0.68259	0.99549	0.89106	0.93711

4 Conclusions

Superhydrophilic composite fibers of Cur-loaded PCL/BSA were fabricated via emulsion electrospinning at different OTW volume ratios (9:1, 8:2, and 7:3). Firstly, stable W/O emulsions were developed by virtue of the superior emulsifying capability of 10% (w/v) BSA, and the droplet diameter increased with the decline of the OTW volume ratio. Subsequently, these emulsions were formulated into Cur-loaded PCL/BSA composite fibers with improved morphology, thermal stability, and hydrophilicity as compared to those of Cur-loaded PCL samples. Moreover, the average diameter of fibers increased as the OTW volume ratio diminished. Particularly, the fibrous membranes with the OTW volume ratio of 7:3 not only presented the highest modulus of elasticity and the largest elongation at break, but also exhibited the most sustained drug release behavior. The release process of Cur was mainly controlled by diffusion. The present study may broaden the applications of PCL materials in biomedical fields.

Declaration of competing interests The authors declare no competing financial interests.

Acknowledgements This work was financially supported by the Basic Research Project of Xuzhou Science and Technology Bureau (KC22004).

Online appendix Electronic supplementary material (ESM) can be found in the online version at https://doi.org/10.1007/s11706-025-0717-0 and https://journal.hep.com.cn/foms/EN/10.1007/s11706-025-0717-0 that includes Figs. S1–S2.

References

[1] Agarwal S, Greiner A. On the way to clean and safe electrospinning-green electrospinning: emulsion and suspension electrospinning. Polymers for Advanced Technologies, 2011, 22(3): 372−378

[2] Avossa J, Herwig G, Toncelli C, et al. Electrospinning based on benign solvents: current definitions, implications and strategies. Green Chemistry, 2022, 24(6): 2347−2375

[3] İnan-Çınkır N, Ağçam E, Altay F, et al. Emulsion electrospinning of zein nanofibers with carotenoid microemulsion: optimization, characterization and fortification. Food Chemistry, 2024, 430: 137005

[4] Ma L, Shi X J, Zhang X X, et al. Electrospinning of polycaprolacton/chitosan core–shell nanofibers by a stable emulsion system. Colloids and Surfaces A: Physicochemical and Engineering Aspects, 2019, 583: 123956

[5] Hemmatian T, Seo K H, Yanilmaz M, et al. The bacterial control of poly (lactic acid) nanofibers loaded with plant-derived monoterpenoids via emulsion electrospinning. Polymers, 2021, 13(19): 3405

[6] Norouzi M R, Ghasemi-Mobarakeh L, Itel F, et al. Emulsion electrospinning of sodium alginate/poly(ε-caprolactone) core/shell nanofibers for biomedical applications. Nanoscale Advances, 2022, 4(13): 2929−2941

[7] Mouro C, Gomes A P, Gouveia I C. Emulsion electrospinning of PLLA/PVA/chitosan with *Hypericum perforatum* L. as an antibacterial nanofibrous wound dressing. GELS, 2023, 9(5): 353

[8] Zhang W, Wang Q Q, Wang K R, et al. Construction of an ornidazole/bFGF-loaded electrospun composite membrane with a core–shell structure for guided tissue regeneration. Materials & Design, 2022, 221: 110960

[9] Wang Y, Yu D G, Liu Y, et al. Progress of electrospun nanofibrous carriers for modifications to drug release profiles. Journal of Functional Biomaterials, 2022, 13(4): 289

[10] Kamali H, Farzadnia P, Movaffagh J, et al. Optimization of curcumin nanofibers as fast dissolving oral films prepared by emulsion electrospinning via central composite design. Journal of Drug Delivery Science and Technology, 2022, 75: 103714

[11] Park J H, Park H J, Tucker S J, et al. 3D printing of poly-ε-caprolactone (PCL) auxetic implants with advanced performance for large volume soft tissue engineering. Advanced Functional Materials, 2023, 33(24): 2215220

[12] Xue X, Zhang H, Liu H, et al. Rational design of multifunctional CuS nanoparticle–PEG composite soft hydrogel-coated 3D hard polycaprolactone scaffolds for efficient bone regeneration. Advanced Functional Materials, 2022, 32(33): 2202470

[13] Pawar R, Pathan A, Nagaraj S, et al. Polycaprolactone and its derivatives for drug delivery. Polymers for Advanced Technologies, 2023, 34(10): 3296−3316

[14] Rajasekaran R, Ojha A K, Seesala V S, et al. Polyaniline doped silk fibroin–PCL electrospunfiber: an electroactive fibrous sheet for full-thickness wound healing study. Chemical Engineering Journal, 2023, 475: 146245

[15] Soleymani F, Shahin N, Emadi R. Cellular behavior and antibacterial properties of MAO/PCL–chitosan–nanobaghdadite composite coating on biodegradable AZ91 alloy. Materials Letters, 2023, 352: 135130

[16] Luginina M, Schuhladen K, Orrú R, et al. Electrospun PCL/PGS composite fibers incorporating bioactive glass particles for soft tissue engineering applications. Nanomaterials, 2020, 10(5): 978

[17] Snyder Y, Todd M, Jana S. Substrates with tunable hydrophobicity for optimal cell adhesion. Macromolecular Bioscience, 2024, 24(11): 2400196

[18] Azimi B, Nourpanah P, Rabiee M, et al. Application of the dry-spinning method to produce poly(ε-caprolactone) fibers containing bovine serum albumin laden gelatin nanoparticles. Journal of Applied Polymer Science, 2016, 133(48): 44233

[19] Yang Z H, Zhang N, Ma T, et al. Engineered bovine serum albumin-based nanoparticles with pH-sensitivity for doxorubicin delivery and controlled release. Drug Delivery, 2020, 27(1): 1156−1164

[20] Rafiei M, Jooybar E, Abdekhodaie M J, et al. Construction of 3D fibrous PCL scaffolds by coaxial electrospinning for protein delivery. Materials Science and Engineering C: Materials for Biological Applications, 2020, 113: 110913

[21] Homaeigohar S, Monavari M, Koenen B, et al. Biomimetic biohybrid nanofibers containing bovine serum albumin as a bioactive moiety for wound dressing. Materials Science and Engineering C: Materials for Biological Applications, 2021, 123: 111965

[22] Valmikinathan C M, Defroda S, Yu X. Polycaprolactone and bovine serum albumin based nanofibers for controlled release of nerve growth factor. Biomacromolecules, 2009, 10(5): 1084−1089

[23] Zhang S, Campagne C, Salaün F. Preparation of electrosprayed poly(caprolactone) microparticles based on green solvents and related investigations on the effects of solution properties as well

as operating parameters. Coatings, 2019, 9(2): 84

[24] Causa A, Filippone G, Acierno D, et al. Surface morphology, crystallinity, and hydrophilicity of poly(ε-caprolactone) films prepared via casting of ethyl lactate and ethyl acetate solutions. Macromolecular Chemistry and Physics, 2015, 216(1): 49−58

[25] Fahimirad S, Abtahi H, Satei P, et al. Wound healing performance of PCL/chitosan based electrospun nanofiber electrosprayed with curcumin loaded chitosan nanoparticles. Carbohydrate Polymers, 2021, 259: 117640

[26] Tao B L, Lin C C, Yuan Z, et al. Near infrared light-triggered on-demand Cur release from Gel-PDA@Cur composite hydrogel for antibacterial wound healing. Chemical Engineering Journal, 2021, 403: 126182

[27] Madeira P P, Rocha I L D, Rosa M E, et al. On the aggregation of bovine serum albumin. Journal of Molecular Liquids, 2022, 349: 118183

[28] Teng S H, Zhu P H, Wang P. Surfactant-free fabrication of curcumin-loaded emulsion coatings on titanium for biomedical applications. Colloids and Surfaces A: Physicochemical and Engineering Aspects, 2024, 685: 133262

[29] Zhou H J, Teng S H, Zhou Y B, et al. Green strategy to develop novel drug-containing poly(ε-caprolactone)–chitosan–silica xerogel hybrid fibers for biomedical applications. Journal of Nanomaterials, 2020, 2020: 6659287

[30] Zupancic S, Preem L, Kristl J, et al. Impact of PCL nanofiber mat structural properties on hydrophilic drug release and antibacterial activity on periodontal pathogens. European Journal of Pharmaceutical Sciences, 2018, 122: 347−358

[31] Teodoro K B R, Alvarenga A D, Oliveria L F R, et al. Fast fabrication of multifunctional PCL/curcumin nanofibrous membranes for wound dressings. ACS Applied Bio Materials, 2023, 6(6): 2325−2337

[32] Chen S C, Huang X B, Cai X M, et al. The influence of fiber diameter of electrospun poly(lactic acid) on drug delivery. Fibers and Polymers, 2012, 13(9): 1120−1125